Computers and Concrete, *Vol. 16, No. 3 (2015) 429-448*
DOI: http://dx.doi.org/10.12989/cac.2015.16.3.429

Dynamic response of concrete gravity dams using different water modelling approaches: westergaard, lagrange and euler

A.C. Altunisik and H. Sesli*

Department of Civil Engineering, Karadeniz Technical University, Trabzon, Turkey

(Received November 21, 2014, Revised July 10, 2015, Accepted August 18, 2015)

Abstract. The dams are huge structures storing a large amount of water and failures of them cause especially irreparable loss of lives during the earthquakes. They are named as a group of structures subjected to fluid-structure interaction. So, the response of the fluid and its hydrodynamic pressures on the dam should be reflected more accurately in the structural analyses to determine the real behavior as soon as possible. Different mathematical and analytical modelling approaches can be used to calculate the water hydrodynamic pressure effect on the dam body. In this paper, it is aimed to determine the dynamic response of concrete gravity dams using different water modelling approaches such as Westergaard, Lagrange and Euler. For this purpose, Sarıyar concrete gravity dam located on the Sakarya River, which is 120km to the northeast of Ankara, is selected as a case study. Firstly, the main principals and basic formulation of all approaches are given. After, the finite element models of the dam are constituted considering dam-reservoir-foundation interaction using ANSYS software. To determine the structural response of the dam, the linear transient analyses are performed using 1992 Erzincan earthquake ground motion record. In the analyses, element matrices are computed using the Gauss numerical integration technique. The Newmark method is used in the solution of the equation of motions. Rayleigh damping is considered. At the end of the analyses, dynamic characteristics, maximum displacements, maximum-minimum principal stresses and maximum-minimum principal strains are attained and compared with each other for Westergaard, Lagrange and Euler approaches.

Keywords: concrete gravity dam; euler; dam-reservoir-foundation interaction; hydrodynamic pressure; lagrange; westergaard

1. Introduction

Dams have contributed to the development of civilization for a long time. They will continue to keep their importance in satisfying the ever increasing demand for power, irrigation and drinking water, the protection of man, property and environments from catastrophic floods, and in regulating the flow of rivers (Akkose and Simsek 2010). Several factors, which affect the dynamic response during earthquake, can be remarked such as interaction of dam-reservoir interaction and consistencies of the hydrodynamic pressures on dam body. Beside these parameters, hydrodynamic pressures acting on dam faces is one of the most important and influential. So, the calculation of

*Corresponding author, Assistant Professor, E-mail: ahmetcan8284@hotmail.com

http://www.techno-press.org/?journal=cac&subpage=8 ISSN: 1598-8198 (Print), 1598-818X (Online)

this parameter is very important especially during dynamic loads such as earthquake.

Some papers can be obtained in literature about the static and dynamic behavior of dams considering dam-reservoir-foundation interaction using different water modelling approaches. Westergaard (1933) carried out the first hydrodynamic analysis on the dam-reservoir system. Samii and Lotfi (2007) performed a study about the comparison of coupled and decoupled modal approaches in seismic analysis for concrete gravity dams. Fathi and Lotfi (2008) investigated the effects of reservoir length on the dynamic analysis of concrete gravity dams. In the analysis, the reservoir is considered by a combination of fluid finite elements and two-dimensional fluid hyper-elements. Bayraktar *et al.* (2009, 2010) aimed to determine the reservoir length effect on seismic performance of gravity dams subjected to near and far fault ground motions. Akköse *et al.* (2010) studied on the nonlinear seismic response of concrete gravity dams subjected to near and far fault ground motions including dam-water-sediment-foundation rock interaction using Lagrangian approach. Wood *et al.* (2010) offered a computational partitioned coupling strategy for the modelling of large deformation fluid-structure interaction. Gogoi and Maity (2010) produced a unique method to evaluate the hydrodynamic pressure on the upstream face in concrete dams due to seismic excitation. Degroote *et al.* (2010) performed a stability analysis of Gauss-Seidel coupling iterations for partitioned simulation of fluid-structure interaction. Sevim *et al.* (2011) presented the water length and height effects on the earthquake behavior of arch dam-reservoir-foundation systems using Lagrangian approach. Heydari and Mansoori (2011) discussed on dam-reservoir interaction modelling approaches using different finite element software's considering dynamics earthquake loads. Shariatmadar and Mirhaj (2011) displayed the dam-reservoir-foundation interaction effects on the modal characteristics of concrete gravity dams. Chen and Yuan (2011) presented a simple approximate formula after hydrodynamic pressure analysis of arch dam. Wang *et al.* (2012) practiced on the nonlinear seismic analyses of concrete gravity dams using 3D dam model considering hydrodynamic effects of the impounded water. Lin *et al.* (2012) developed an efficient approach for the hydrodynamic analysis of dam–reservoir systems. Miquel and Bouaanani (2013) proposed a new practical and efficient procedure to investigate the seismic response of gravity dams. Samii and Lotfi (2013) studied on the absorbing boundary conditions for dynamic analysis. Wick (2013) carried out a study about the coupling of fully eulerian and arbitrary lagrangian-eulerian methods for fluid-structure interaction computations. From these studies, it is seen that there is no enough studies about the determination and comparison of dynamic response of gravity dams using different reservoir modelling approaches such as Westergaard, Lagrange and Euler.

This paper present the dynamic response of concrete gravity dams using different water modelling approaches such as Westergaard, Lagrange and Euler. Sarıyar concrete gravity dam is selected for application. The finite element models of the dam are constituted considering dam-reservoir-foundation interaction. To determine the structural response of the dam, the linear transient analyses are performed using 1992 Erzincan earthquake ground motion record. From the analyses, dynamic characteristics, maximum displacements, maximum-minimum principal stresses and maximum-minimum principal strains are attained and compared with each other for Westergaard, Lagrange and Euler approaches.

2. Formulation

2.1 Westergaard (Added Mass) approach

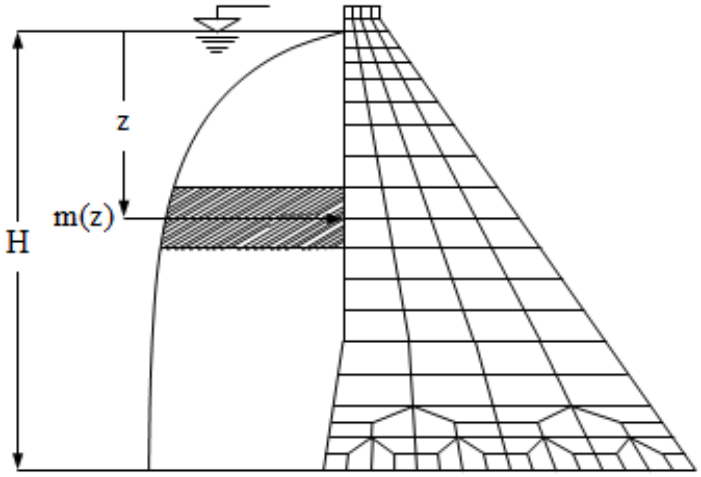

Fig. 1 Distribution of the hydrodynamic pressure on finite mesh

Added mass approach is firstly presented by Westergaard in 1933. In this approach, the dam is accepted as rigid, semi-infinite and have vertical upstream surface. Surface waves in fluid are neglected. The distribution of hydrodynamic pressure occurred along upstream surface after earthquake takes into account as mass distribution pulsed with the dam. Individual masses calculated with distribution of hydrodynamic pressure are added on the nodes of the finite element mesh along upstream surface of the dam. Fig. 1 shows the changing of water mass according to the depth.

Individual masses are given according to the Fig. 1 as following

$$m(z) = \frac{7}{8}\frac{w}{g}\sqrt{Hz} \tag{1}$$

where $m(z)$, w, g, H and z are distribution of mass depend on depth of reservoir water, unit weight of water, acceleration of gravity and depth of water as from surface, respectively.

2.2 Lagrange approach

In the Lagrange approach, the response of the dam and reservoir is expressed with displacements. For using same variables, specific interface equations are not essential (Calayır 1994, Calayır 1996). The formulation of the fluid system based on the Lagrange approach can be found in literature (Wilson and Khalvati 1983). In this approach, the fluid is assumed to be linearly elastic, inviscid and with irrotational flow field. For a general three-dimensional fluid, stress-strain relationships can be written in matrix form as follows

$$\begin{Bmatrix} P \\ P_x \\ P_y \\ P_z \end{Bmatrix} = \begin{bmatrix} C_{11} & 0 & 0 & 0 \\ 0 & C_{22} & 0 & 0 \\ 0 & 0 & C_{33} & 0 \\ 0 & 0 & 0 & C_{44} \end{bmatrix} \begin{Bmatrix} \varepsilon_v \\ w_x \\ w_y \\ w_z \end{Bmatrix} \tag{2}$$

In this equation, P_x, P_y, P_z are the rotational stresses; C_{22}, C_{33}, C_{44} are the constraint parameters and wx, wy and wz are the rotations about the cartesian axis x, y and z, respectively, where P, C_{11}, and ε_v are the pressures which are equal to mean stresses, the bulk modulus and the volumetric strains of the fluid, respectively. Since irrotationality of the fluid is considered like penalty methods (Bathe 1996), rotations and constraint parameters are included in the stress-strain equation (Eq. (2)) of the fluid.

In this study, the equations of motion of the fluid system were obtained using potential and kinetic energy principles. Using the finite element method, the total strain energy of the fluid system may be written as

$$\pi_e = \frac{1}{2}\mathbf{U}_f^T\mathbf{K}_f\mathbf{U}_f \tag{3}$$

where $\mathbf{U}_f$ and $\mathbf{K}_f$ are the vectors of nodal displacements and the stiffness matrix of the fluid system, respectively. $\mathbf{K}_f$ is obtained by summing the stiffness matrices of the fluid elements in the following

$$\left.\begin{aligned}\mathbf{K}_f &= \sum \mathbf{K}_f^e \\ \mathbf{K}_f^e &= \int_V \mathbf{B}_f^{eT}\mathbf{C}_f\mathbf{B}_f^e dV^e\end{aligned}\right\} \tag{4}$$

where $\mathbf{C}_f$ is the elasticity matrix consisting of diagonal terms in Eq. (2). $\mathbf{B}_f^e$ is the strain-displacement matrix of the fluid element.

An important behavior of fluid systems is the ability to displace without a change in volume. For reservoir and storage tanks, this movement is known as sloshing waves in which the displacement is in the vertical direction. The increase in the potential energy of the system due to the free surface motion can be written as

$$\pi_s = \frac{1}{2}\mathbf{U}_{sf}^T\mathbf{S}_f\mathbf{U}_{sf} \tag{5}$$

where $\mathbf{U}_{sf}$ and $\mathbf{S}_f$ are the vertical nodal displacement vector and the stiffness matrix of the free surface of the fluid system, respectively. $\mathbf{S}_f$ is obtained by the sum of the stiffness matrices of the free surface fluid elements in the following

$$\left.\begin{aligned}\mathbf{S}_f &= \sum \mathbf{S}_f^e \\ \mathbf{S}_f^e &= \rho_f g\int_A \mathbf{h}_s^T\mathbf{h}_s dA^e\end{aligned}\right\} \tag{6}$$

where $\mathbf{h}_s$ is the vector consisting of interpolation functions of the free surface fluid element. ρf and g are the mass density of the fluid and the acceleration due to gravity, respectively. Also, the kinetic energy of the system can be written as

$$T = \frac{1}{2}\dot{\mathbf{U}}_f^T\mathbf{M}_f\dot{\mathbf{U}}_f \tag{7}$$

where $\dot{\mathbf{U}}_f$ and $\mathbf{M}_f$ are the nodal velocity vector and the mass matrix of the fluid system, respectively. $\mathbf{M}_f$ can be obtained by summing the mass matrices of the fluid elements in the following

$$\left.\begin{aligned}\mathbf{M}_f &= \sum \mathbf{M}_f^e \\ \mathbf{M}_f^e &= \rho_f \int_V \mathbf{H}^T \mathbf{H} dV^e\end{aligned}\right\} \tag{8}$$

where $\mathbf{H}$ is the matrix consisting of interpolation functions of the fluid element. If Eqs. (3), (5) and (7) are combined using the Lagrange's equation (Clough and Penzien, 1975); the following set of equations is obtained

$$\mathbf{M}_f \ddot{\mathbf{U}}_f + \mathbf{K}_f^* \mathbf{U}_f = \mathbf{R}_f \tag{9}$$

where $\mathbf{K}_f^*$, $\ddot{\mathbf{U}}_f$ and $\mathbf{R}_f$ are the system stiffness matrix including the free surface stiffness, the nodal acceleration vector and time-varying nodal force vector for the fluid system, respectively. In the formation of the fluid element matrices, reduced integration orders were utilized.

The equations of motion of the fluid system, Eq. (9), have a similar form with those of the structural system. To obtain the coupled equations of the fluid-structure system, the determination of the interface condition is required. Because the fluid is assumed to be inviscid, only the displacement in the normal direction to the interface is continuous at the interface of the system. Assuming that the positive face is the structure and the negative face is the fluid, the boundary condition at the fluid-structure interface is

$$U_n^- = U_n^+ \tag{10}$$

where U_n is the normal component of the interface displacement (Akkas *et al*. 1979). Using the interface condition, the equations of motion of the coupled system to ground motion including damping effects are given by

$$\mathbf{M}_c \ddot{\mathbf{U}}_c + \mathbf{C}_c \dot{\mathbf{U}}_c + \mathbf{K}_c \mathbf{U}_c = \mathbf{R}_c \tag{11}$$

in which $\mathbf{M}_c$, $\mathbf{C}_c$, and $\mathbf{K}_c$ are the mass, damping and stiffness matrices for the coupled system, respectively. $\mathbf{U}_c$, $\dot{\mathbf{U}}_c$, $\ddot{\mathbf{U}}_c$ and $\mathbf{R}_c$ are the vectors of the displacements, velocities, accelerations and external loads of the coupled system, respectively.

2.3 Euler approach

Euler approach is widely used in the finite and boundary element analysis for dams considering fluid-structure interaction. In this approach, the structure and fluid motions are expressed with displacements and pressures, respectively. Structure and fluid moves together based on fluid-structure interface. Hence, specific interface equations must be identified.

Three dimensional motion of a linear compressible, nonviscous and nonrotational fluid under small displacements are given as wave equation in literature (Cook *et al*. 1989, Zeinkiewicz and Taylor 1991)

$$P_{,xx} + P_{,yy} + P_{,zz} = \frac{1}{C^2} P_{,tt} \tag{12}$$

where x, y and z are cartesian coordinates. T, C and expressed as time, pressure wave velocity of fluid and second derivative of hydrodynamic pressure for variable i, respectively. Hydrodynamic pressures formed by any effect in fluid are obtained from appropriate boundary conditions for Eq. (12). This boundary conditions

$$P = 0 \quad \text{(if not surface waves on free surface)} \tag{13}$$

$$P = \rho g u_{sf} \quad \text{(if there are surface waves on free surface)} \tag{14}$$

$$P_{,n} = \rho \ddot{u}_n \quad \text{(for fluid-structure interface)} \tag{15}$$

where ρ, g, n, $\ddot{u}_n$ and u_{sf} are mass density of fluid, gravity acceleration, normal to fluid surface for fluid-structure interface, acceleration in direction of normal and displacement of fluid free surface in vertical direction.

Fluid surface waves are negligible in the solutions (Chopra 1967), but these waves are considered the effect of surface waves in this study. Then, the finite element equation of motion for the fluid system

$$\left[M_f^p\right]\left\{\ddot{P}\right\} + \left[K_f^p\right]\{P\} = -\rho\,[R]^T\left\{\ddot{U}_{fs}\right\} \tag{16}$$

where $\left[M_f^p\right]$, $\left\{\ddot{P}\right\}$, $\left[K_f^p\right]$, $\{P\}$, $[R]$ and $\left\{\ddot{U}_{fs}\right\}$ are mass matrix, second derivative of hydrodynamic pressure vector for time, stiffness matrix, hydrodynamic pressure vector, matrix for fluid-fluid interface and structure accelerations in fluid-structure interface, respectively. Finite element equations for dynamic motion of medium

$$[M_s]\left\{\ddot{U}_s\right\} + [C_s]\left\{\dot{U}_s\right\} + [K_s]\{U_s\} = \{F\} + \{F_{fs}\} \tag{17}$$

where $[M_s]$, $[C_s]$, $[K_s]$, $\left\{\ddot{U}_s\right\}$, $\left\{\dot{U}_s\right\}$, $\{U_s\}$, $\{F\}$ and $\{F_{fs}\}$ are mass matrix, damping matrix, stiffness matrix, acceleration vector, velocity vector, displacement vector, external load vector and additional external load vector on structure for hydrodynamic pressures occurred in fluid, respectively. $\{F_{fs}\}$ is expressed and the equations of motion for fluid-structure system are expressed.

$$\{F_{fs}\} = [R]\{P\} \tag{18}$$

$$\begin{bmatrix}[M_s] & [0]\\ [M_{fs}] & \left[M_f^p\right]\end{bmatrix}\begin{Bmatrix}\left\{\ddot{U}_s\right\}\\ \left\{\ddot{P}\right\}\end{Bmatrix} + \begin{bmatrix}[C_s] & [0]\\ [0] & [0]\end{bmatrix}\begin{Bmatrix}\left\{\dot{U}_s\right\}\\ \left\{\dot{P}\right\}\end{Bmatrix} + \begin{bmatrix}[K_s] & [K_{fs}]\\ [0] & \left[K_f^p\right]\end{bmatrix}\begin{Bmatrix}\{U_s\}\\ \{P\}\end{Bmatrix} = \begin{Bmatrix}\{F\}\\ \{0\}\end{Bmatrix} \tag{19}$$

$$\{M_{fs}\} = \rho\,[R]^T \tag{20}$$

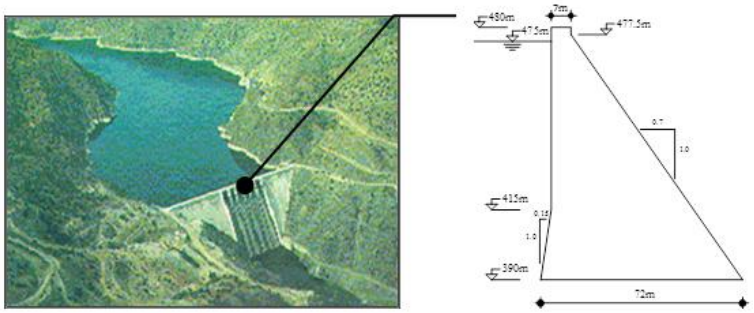

Fig. 2 Sarıyar concrete gravity dam

$$\{K_{fs}\} = -[R] \tag{21}$$

3. Numerical example

The focus of this paper is to determine and compare the structural dynamic behavior of concrete gravity dams including dam-reservoir-foundation interaction using different water modelling approaches such as Westergaard (added masses), Lagrange (displacement-based) and Euler (pressure-based) to imply the hydrodynamic pressure. Sarıyar concrete gravity dam (Fig. 2(a)) is chosen as an application. Sarıyar dam is located on the Sakarya River, 120 km to the northeast of Ankara, in Turkey. The dam is constructed to supply the electric power. The crest length and width are 257 m and 7 m, respectively. Maximum reservoir height is 85 m. The dimensions of the dam are given in Fig. 2(b).

The finite element models of the dam including dam-reservoir-foundation interaction using Westergaard, Lagrange and Euler approaches are constituted in ANSYS program and given in Figs. 3(a)-3(c), respectively. In these models, dam body and foundation are represented by solid elements. Reservoir effect is represented by using added masses on dam body for Westergaard approach. But, in the Lagrange and Euler approaches, fluid elements are used to define the reservoir water and its hydrodynamic pressures. It can be easily seen from the Fig. 3 that the modelling of the water using Westergaard approach is very simply. Only additional masses are defined at special nodes. When the all approaches compared with each other, it is seen that modelling of the water using Lagrange and Euler approaches more difficult from the Westergaard approach. But, there is not any difference between Lagrange and Euler approaches. Only, element type and structural options should be changed to obtain the good and reliable solutions. In the finite element model, Plane182 element is used for dam body and foundation. Also, MASS21, Fluid79 and Fluid29 (structure absent) elements are selected to represent the reservoir water for Westergaard, Lagrange and Euler Approaches, respectively.

Massless foundation is used in all dam-reservoir-foundation models. At the dam-reservoir and reservoir-foundation interface, coupling elements with length of 0.001 m is used to hold the displacements equal between two reciprocal nodes for Lagrange approach. Between the dam and reservoir faces, the thickness of Fluid 29 element, which shows the hydrodynamic pressures effect on dam body, is chosen as 3.125 m for Euler approach. The length of the reservoir in the upstream

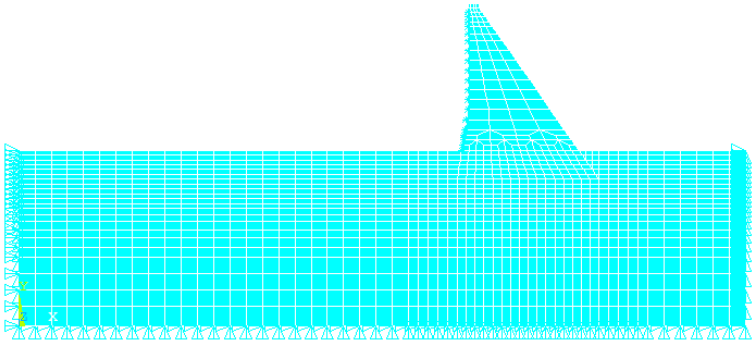

(a) Westergaard approach

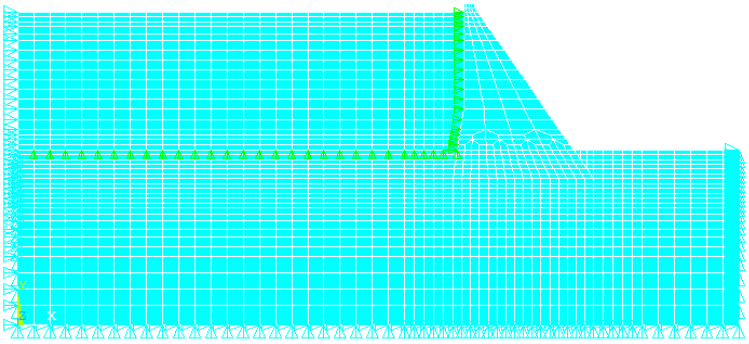

(b) Lagrange approach

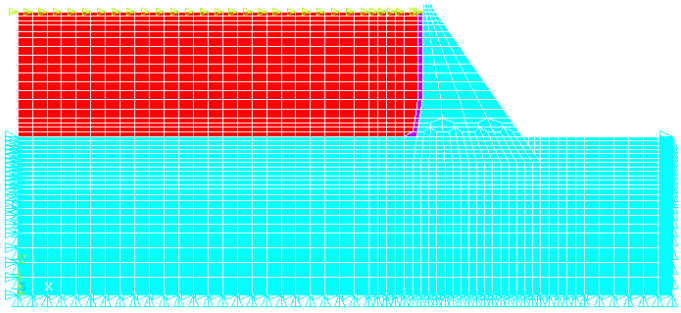

(c) Euler approach

Fig. 3 Two dimensional finite element models of Sarıyar concrete gravity dam including dam-reservoir-foundation systems using Westergaard, Lagrange and Euler approaches

direction is taken to be as much as three times the dam height in all models. It is assumed that the reservoir has constant depth. In addition, foundation depths are taken into account as much as the dam heights. In the upstream direction, foundation length is considered as the reservoir length and in the downstream direction, foundation length is considered as the dam height (Bayraktar *et al.* 2008, Bayraktar *et al.* 2010, Sevim *et al.* 2011a,b). Element matrices are computed using the Gauss numerical integration technique (Bathe 1996). The Newmark method is used in the solution of the equation of motions. Rayleigh damping is considered in the analyses and damping ratio is selected as 5%.

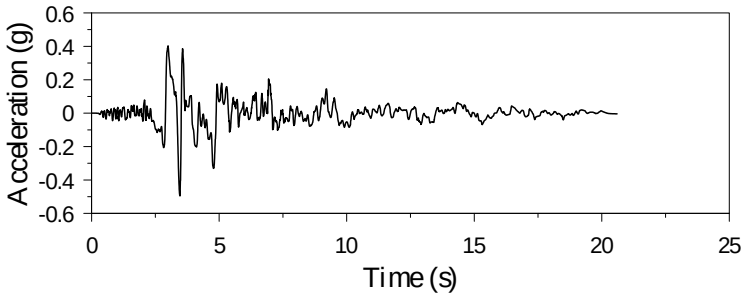

Fig. 4 The time history of the 1992 Erzincan earthquake strong ground motion

Table 1 The material properties used in the analyses

Material	Material Properties		
	Modulus of elasticity (N/m)	*Poisson's ratio (-)*	*Mass per unit vol. (kg/m3)*
Dam (Concrete)	35.0E9	0.15	2400
Foundation	30.0E9	0.2	-
Reservoir	20.7E8	-	1000

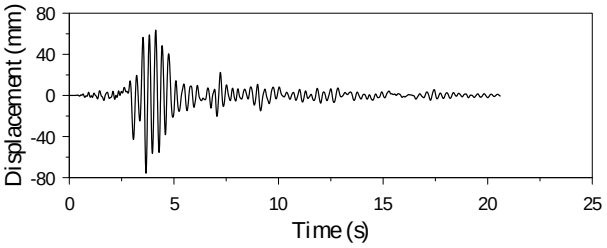

(a) Westergaard approach

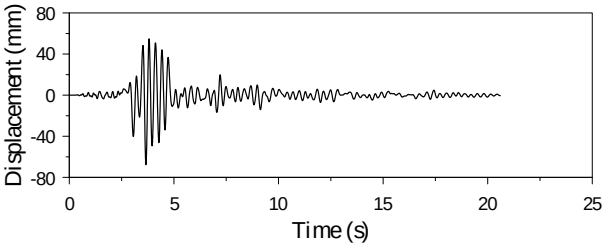

(b) Lagrange approach

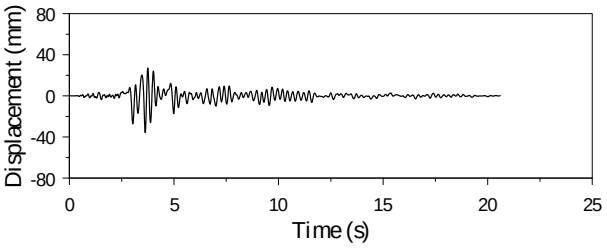

(c) Euler approach

Fig. 5 The time histories of horizontal displacements at the crest point for Westergaard (a) Lagrange (b) and Euler (c) approaches

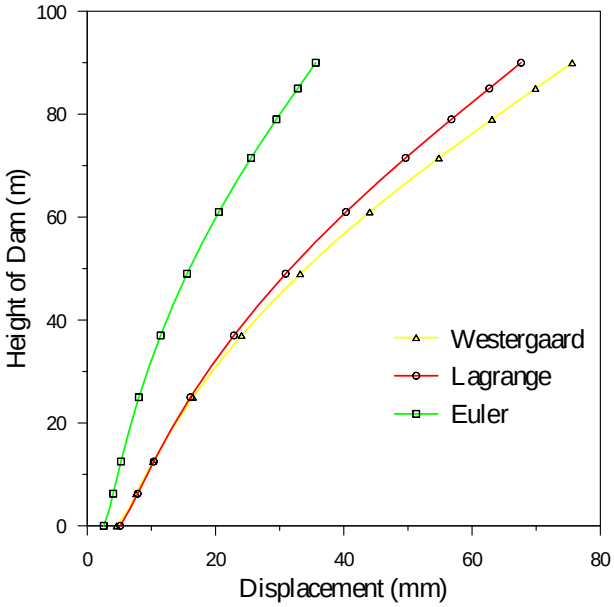

Fig. 6 Maximum horizontal displacements by height of Sarıyar concrete gravity dam

The material properties used in the analyses is given in Table 1. The ERZIKAN/ERZ-EW component of the Erzincan earthquake occurred on March 13, 1992, Erzincan, Turkey is chosen as strong earthquake ground motion record (Fig. 4).

3.1 Displacements

The time histories of the horizontal displacements (upstream-downstream direction) at the crest point of Sarıyar concrete gravity dam obtained from linear transient analysis for three different approaches under ERZIKAN/ERZ-EW component of Erzincan Earthquake (1992) ground motion is presented Figs. 5(a)-5(c). The maximum displacements are attained as 75.61 mm, 67.63 mm and 35.62 mm for Westergaard, Lagrange and Euler approaches, respectively.

The changing of maximum displacements by the height of dam body for Westergaard, Lagrange and Euler approaches are given in Fig. 6. It is clearly seen from the figure that the displacements increase by height of the dam body for all modelling approaches and maximum displacements attained for Westergaard model. The maximum horizontal displacements contours for all approaches are shown in Figs. 7(a)-7(c). This represents the distribution of the peak values reached by the maximum displacement at each point within the sections.

3.2 Principal stresses

The changing of maximum compressive and tensile principal stresses by the height of dam body for Westergaard, Lagrange and Euler approaches are given in Fig. 8. It is seen from the figure that the maximum values of both principle stresses are attained at 3.215 m height from the base point of the dam body. The time histories of the maximum and minimum principal stresses (at 3.125 m) for each approaches are plotted in Figs. 9(a)-9(c). The maximum tensile stresses are

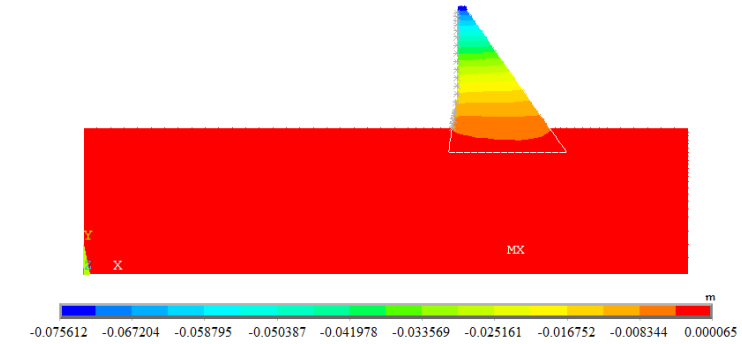

(a) Westergaard approach

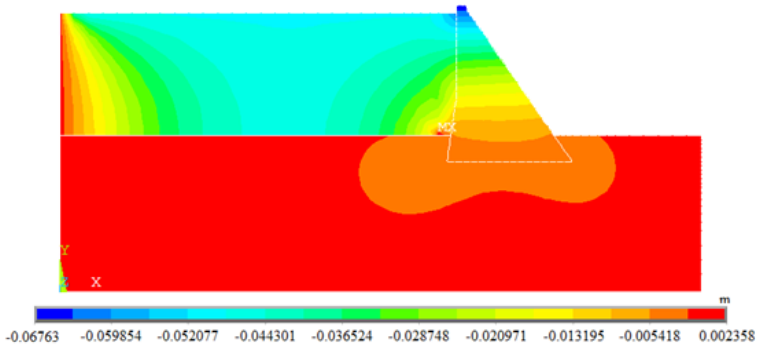

(b) Lagrange approach

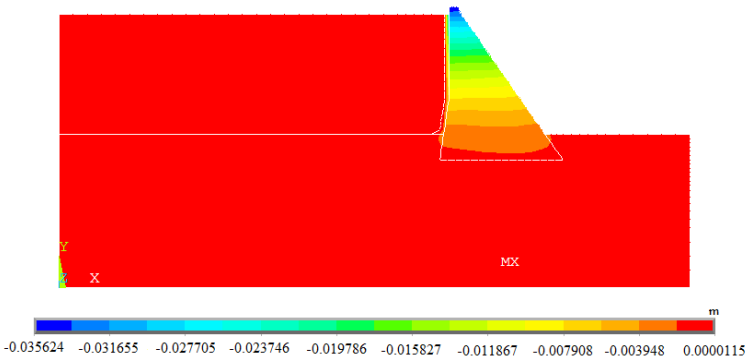

(c) Euler approach

Fig. 7 Maximum displacement contours of the dam-reservoir-foundation system for Westergaard (a) Lagrange (b) and Euler (c) approaches

attained as 12.57MPa, 12.37MPa, 5.30MPa; the maximum compressive stresses are attained as 14.58 MPa, 15.50 MPa, 6.81 MPa for Westergaard, Lagrange and Euler approaches, respectively.

The maximum stresses contours are shown in Figs. 10(a)-11(c). This represents the distribution of peak values reached by maximum stresses at each point within the sections.

3.3 Principal strains

The changing of maximum compressive and tensile principal strains by the height of dam body

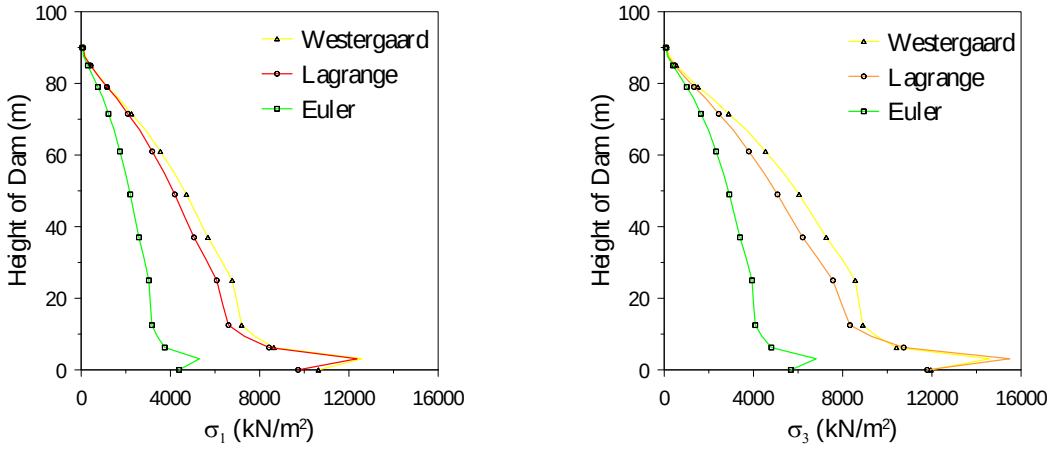

Fig. 8 Changing of maximum tensile (a) and compressive (b) principal stresses by height of the changing Sarıyar concrete gravity dam

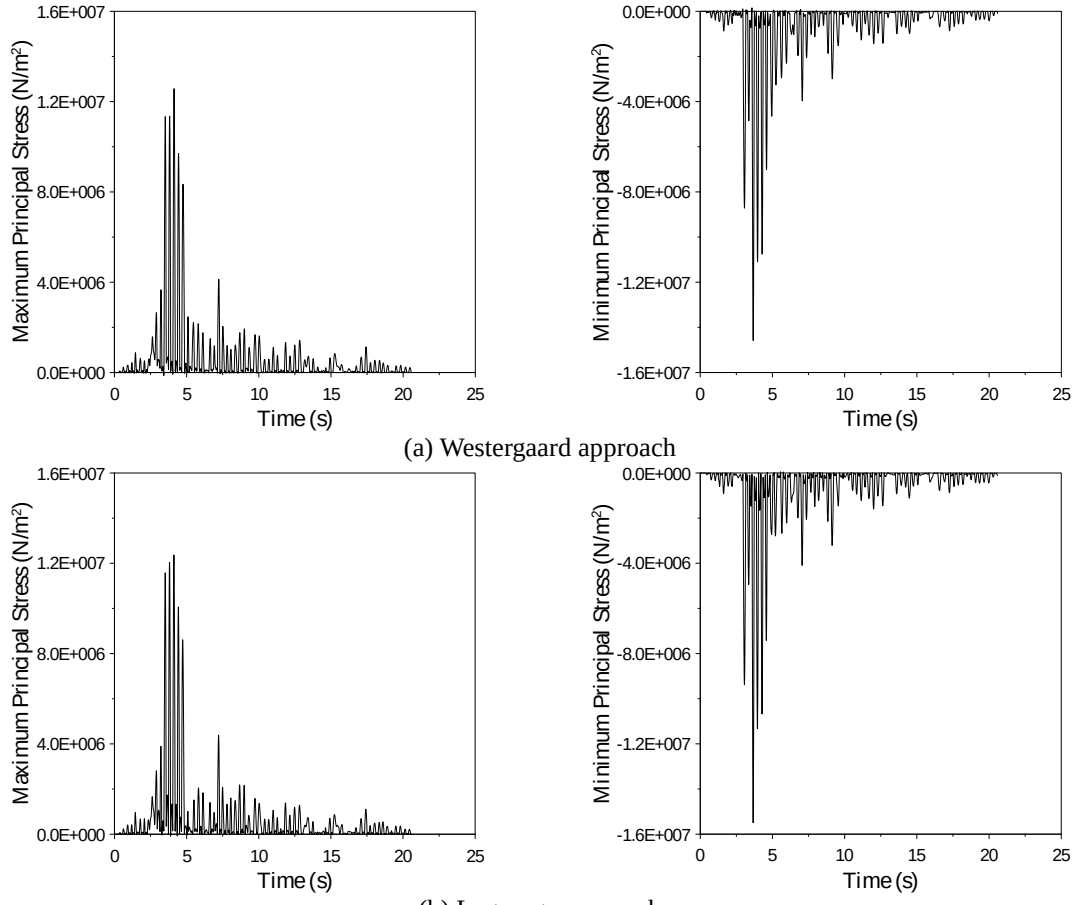

Fig. 9 The time histories of maximum and minimum principal stresses at the 3.125 m Westergaard (a), Lagrange (b) and Euler (c) approaches

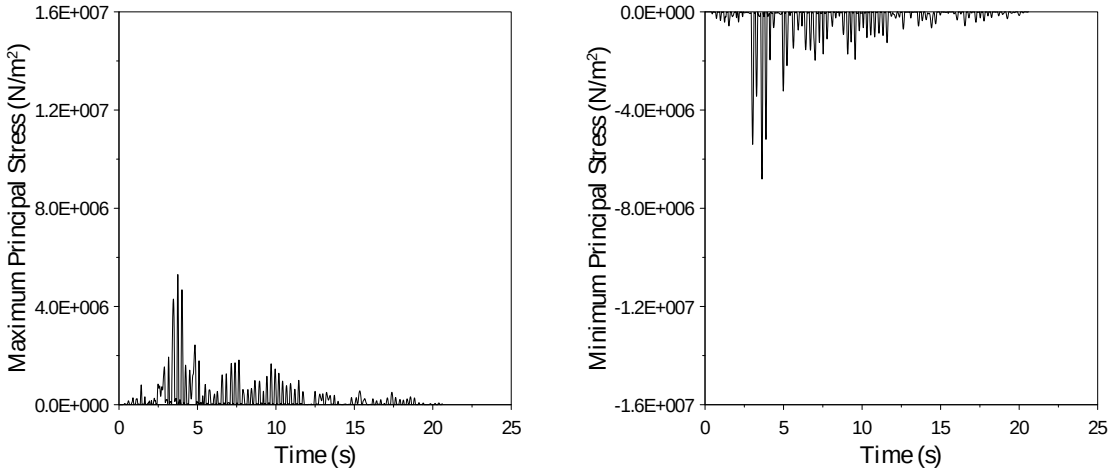

(c) Euler approach

Fig. 9 Continued

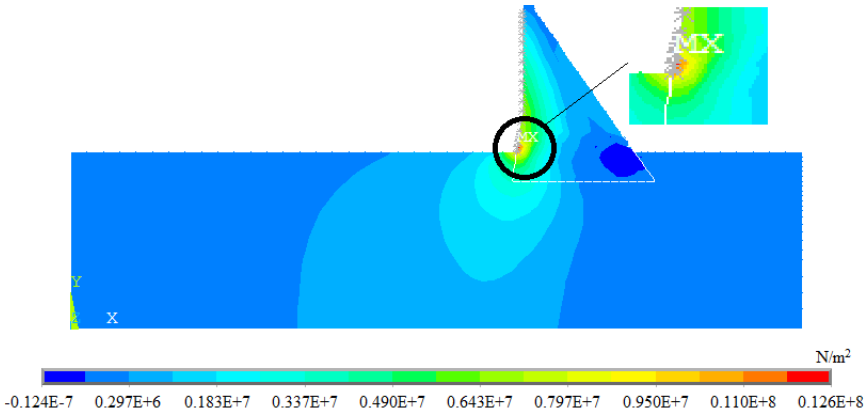

(a) Westergaard approach

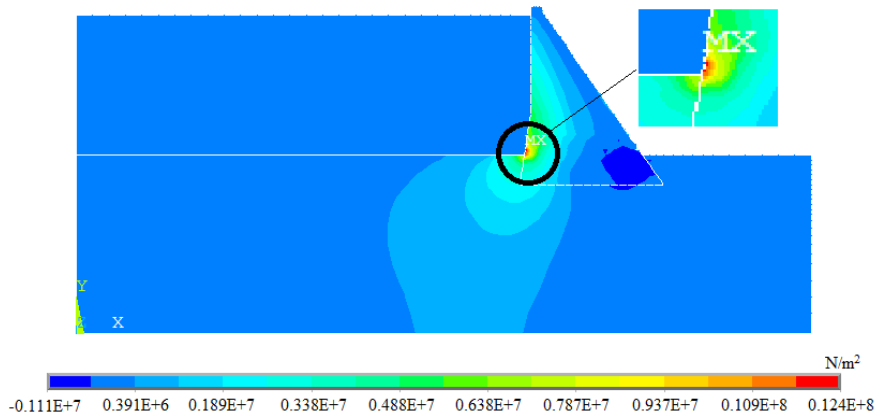

(b) Lagrange approach

Fig. 10 Maximum compressive principle stresses contours of the dam-reservoir-foundation system for Westergaard (a), Lagrange (b) and Euler (c) approaches

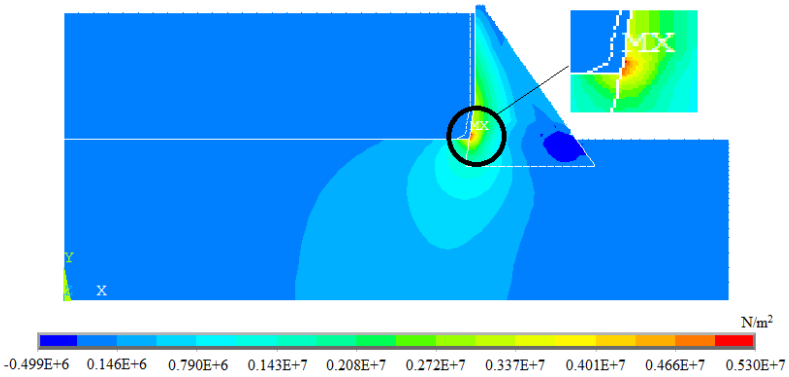

(c) Euler approach

Fig. 10 Continued

for Westergaard, Lagrange and Euler approaches are given in Fig. 12. It is seen from the figure that the maximum values of both principle strains are attained at 3.215 m height from the base point of the dam body. The time histories of the maximum and minimum principal strains (at 3.125 m) for

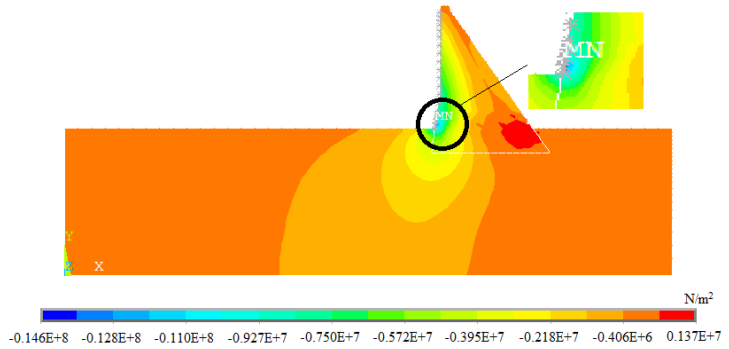

(a) Westergaard approach

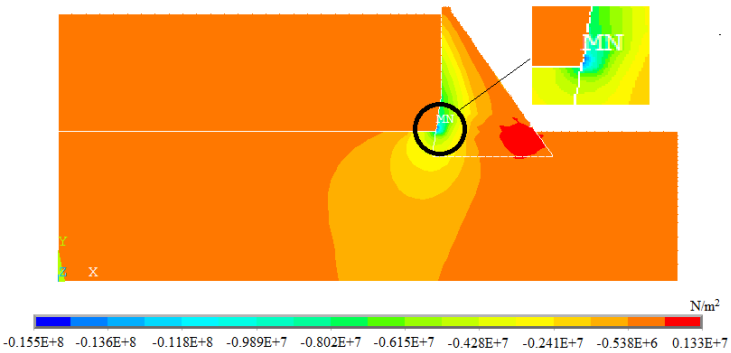

(b) Lagrange approach

Fig. 11 Maximum tensile principle stresses contours of the dam-reservoir-foundation system for Westergaard (a), Lagrange (b) and Euler (c) approaches

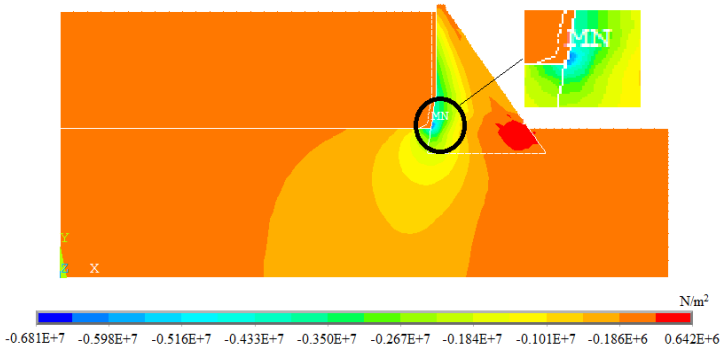

(c) Euler approach

Fig. 11 Continued

Table 2 The maximum values of displacements, maximum-minimum principal stresses and strains

Material	Water modelling approaches		
	Westergaard	*Lagrange*	*Euler*
Displacement	75.61 mm	67.63 mm	35.62 mm
Maximum compressive stresses	14.58 MPa	15.50 MPa	6.81 MPa
Maximum tensile stresses	12.57 MPa	12.37 MPa	5.30 MPa
Maximum compressive strains	41.04E-5	44.13E-5	19.15E-5
Maximum tensile strains	35.47E-5	35.35E-5	14.90E-5

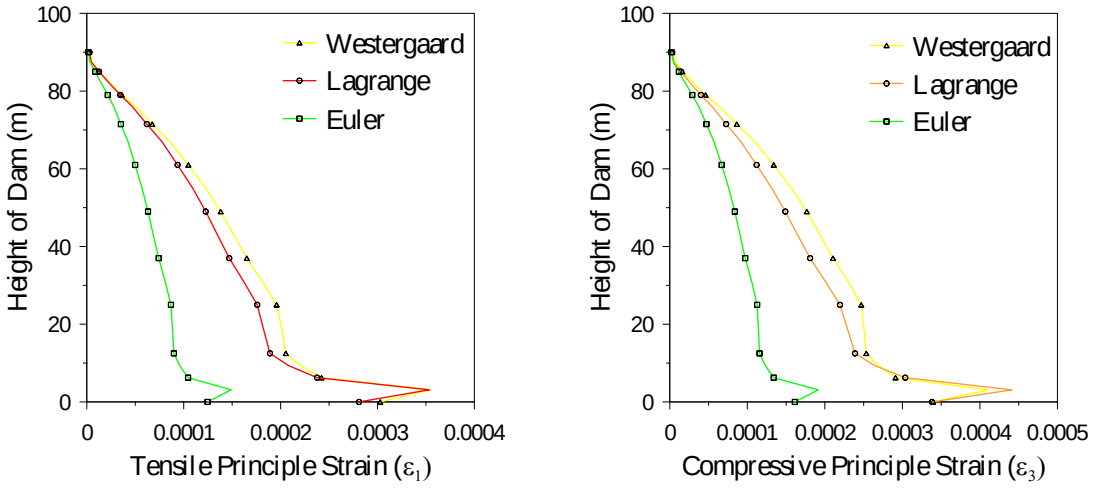

(a) (b)

Fig. 12 Changing of maximum tensile (a) and compressive (b) principal strains by height of the changing Sarıyar concrete gravity dam

each approaches are plotted in Figs. 13(a)-13(c). The maximum tensile and compressive strains are attained as 35.47E-5, 35.35E-5, 14.90E-5; 41.04E-5, 44.13E-5, 19.15E-5 for all approaches, respectively.

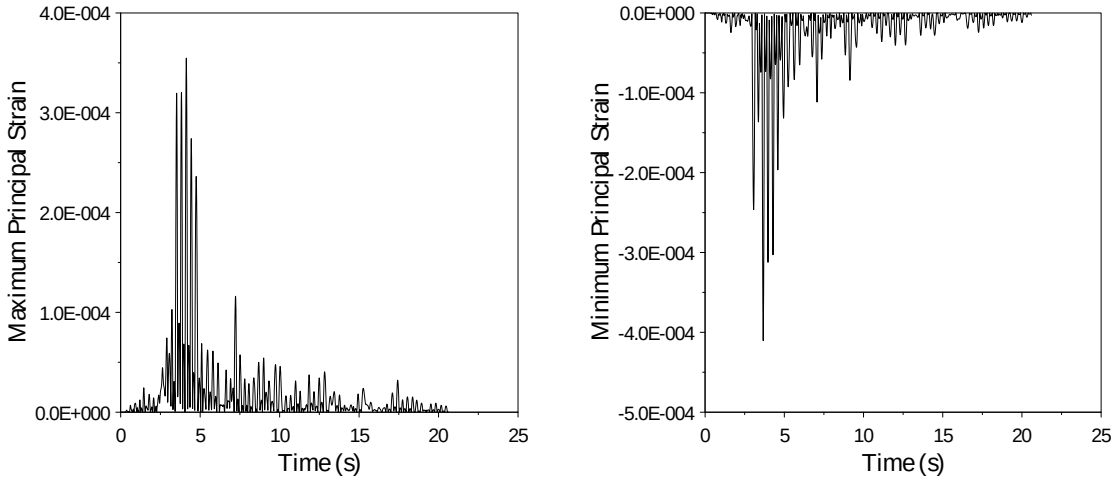

(a) Westergaard approach

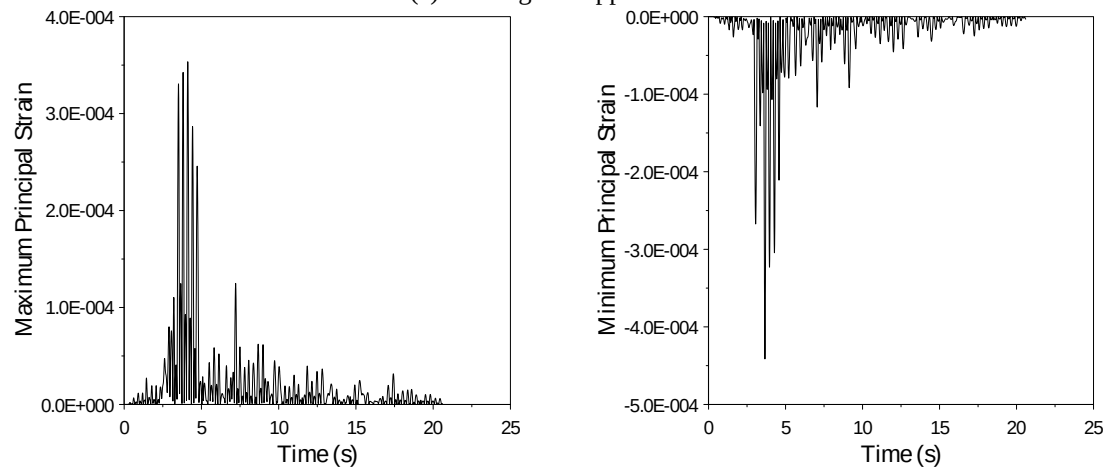

(b) Lagrange approach

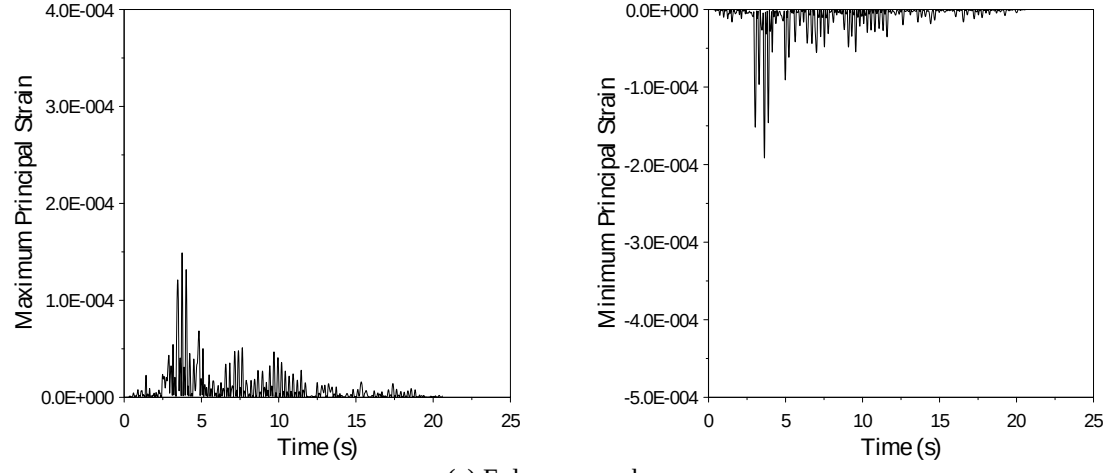

(c) Euler approach

Fig. 13 The time histories of maximum and minimum principal strains at the 3.125 m Westergaard (a), Lagrange (b) and Euler (c) approaches

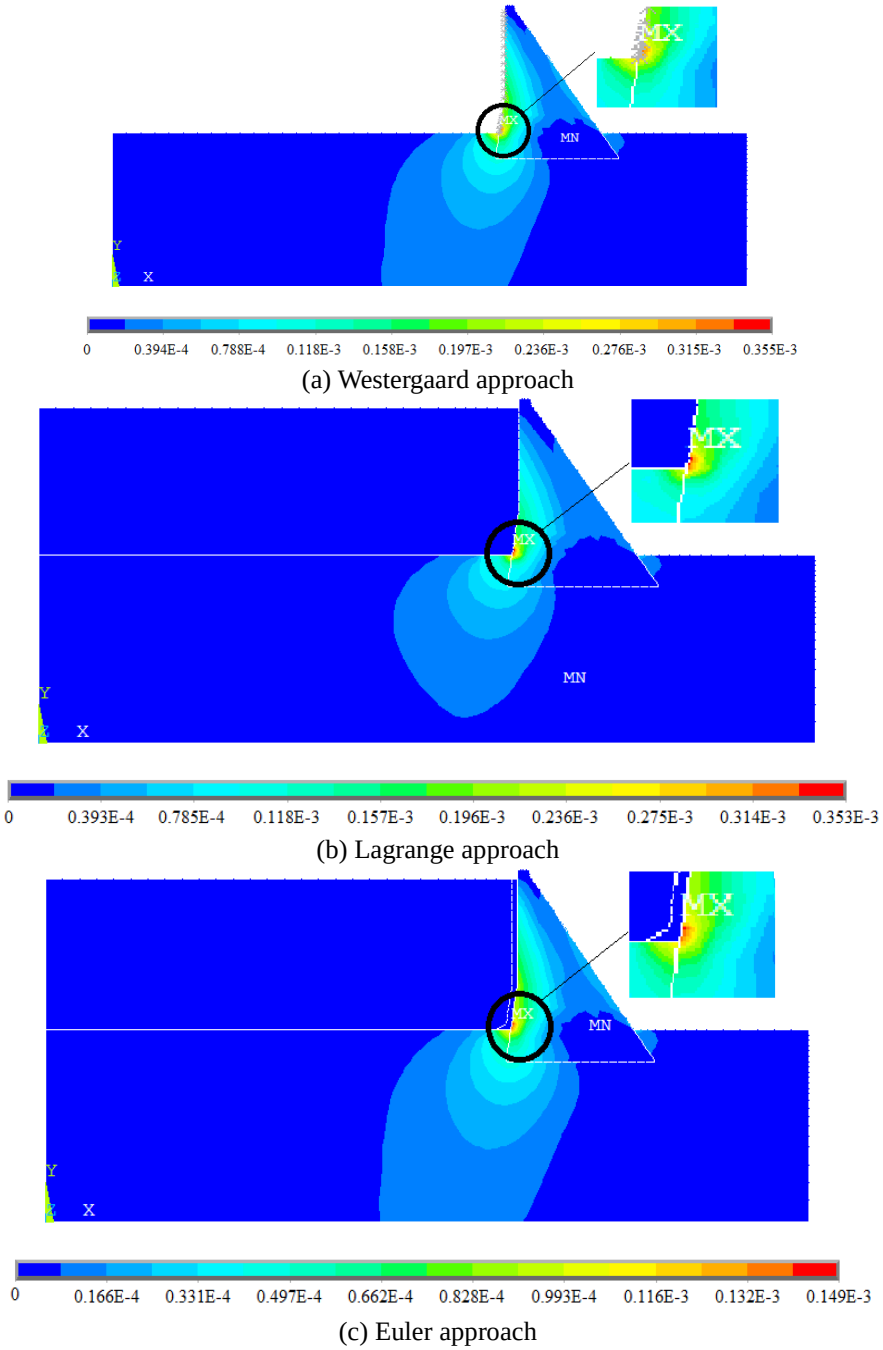

Fig. 14 Maximum compressive principle strains contours of the dam-reservoir-foundation system for Westergaard (a), Lagrange (b) and Euler (c) approaches

The maximum strains contours are shown in Figs. 14(a)-15(c). This represents the distribution of peak values reached by maximum strains at each point within the sections.

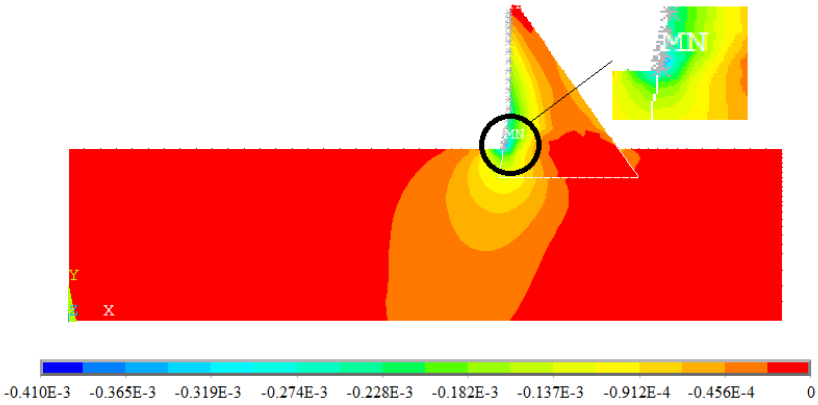

(a) Westergaard approach

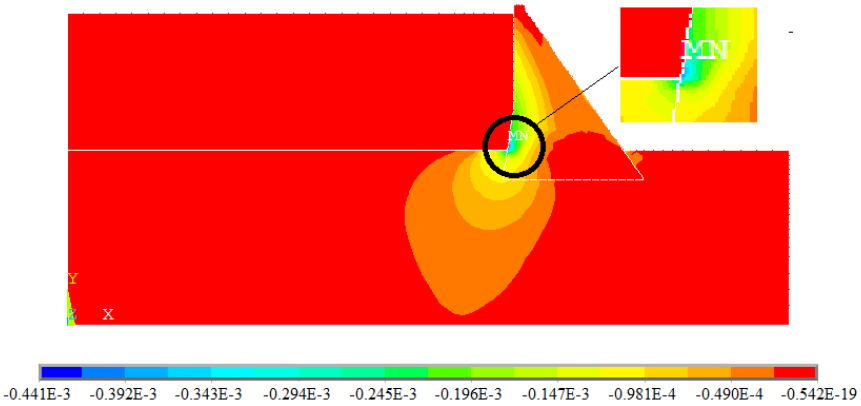

(b) Lagrange approach

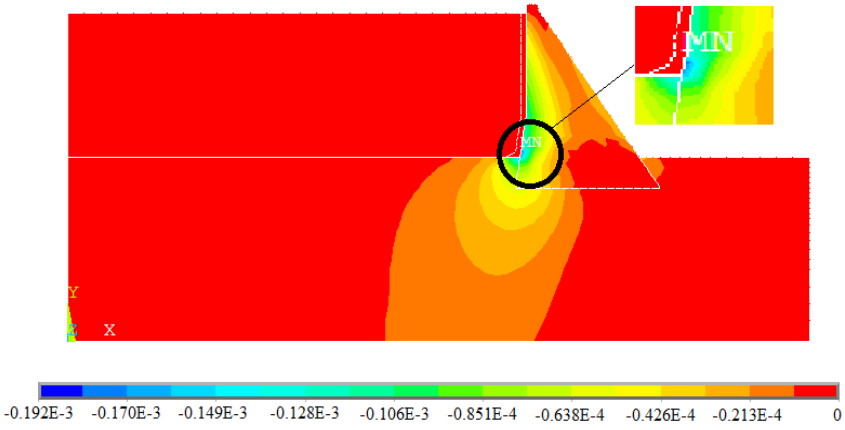

(c) Euler approach

Fig. 15 Maximum tensile principle strains contours of the dam-reservoir-foundation system for Westergaard (a), Lagrange (b) and Euler (c) approaches

The maximum values of displacements, maximum and minimum principal stresses and strains are given in Table 2 to better understanding.

4. Conclusions

This paper present the determination and comparison of dynamic response of concrete gravity dams using different water modelling approaches such as Westergaard, Lagrange and Euler. Sarıyar concrete gravity dam located on in Ankara, Turkey, is selected as a case study. The finite element models of the dam are constituted considering dam-reservoir-foundation interaction for all reservoir models. Comparing the results of this study, the following observations can be made:

- The displacements increase by the height of the dam body and maximum displacements occur at crest points for each reservoir modelling approaches. Maximum and minimum displacements are attained from Westergaard and Euler approaches, respectively.
- Maximum compressive and tensile principal stresses and strains have a decreasing trend from the base to crest point of the dam body for all reservoir modelling approaches. Maximum stresses and strains are occurred at the 3.125 m height from the base for Westergaard, Lagrange and Euler approaches.
- It is seen that maximum and minimum principal stresses and strains are nearly equal for Westergaard and Lagrange approaches. But, the values attained from Euler approach are different and quite lower than the others.
- MASS21 element type, coupling lines and FLUID29 element using structure present options can be considered to dam-reservoir and reservoir-foundation interaction in Westergaard, Lagrange and Euler approaches, respectively.

All approaches are suggested, published and used nearly all researchers (related to dam-reservoir-foundation interaction). It can be said from the study parallel to literature that more general results can be obtained with Westergaard approach. Besides, Lagrange and Euler approaches can be used to determine/attain the real behavior of dam structures.

References

Akkaş, N., Akay, H.U. and Yılmaz, C.(1979), "Applicability of general-purpose finite element programs in solid-fluid interaction problems", *Comput. Struct.*, **10**(5), 773-783.

Akköse, M. and Şimşek, E. (2010), "Non-linear seismic response of concrete gravity dams to near-fault ground motions including dam-water-sediment-foundation interaction", *Appl. Math. Model.*, **34**(11), 3685-3700.

Bathe, K.J. (1996), "Finite Element Procedures in Engineering Analysis", Englewood Cliffs, New Jersey, Prentice-Hall.

Bayraktar, A., Altunışık, A.C., Sevim, B., Kartal, M.E. and Türker, T. (2008), "Near-fault ground motion effects on the nonlinear response of dam-reservoir-foundation systems", *Struct. Eng. Mech.*, **28**(4), 411-442.

Bayraktar, A., Altunişik, A.C., Sevim, B., Kartal, M.E, Türker, T. and Bilici, Y. (2009), "Comparison of near- and far-fault ground motion effect on the nonlinear response of dam-reservoir-foundation systems", *Nonlinear. Dynam.*, **58**(4), 655-673.

Bayraktar, A., Türker, T., Akköse, M. and Ateş, Ş. (2010), "The effect of reservoir length on seismic performance of gravity dams to near- and far-fault ground motions", *Nat. Hazards.*, **52**(2), 257-275.

Calayır, Y. (1994), " Dynamic Analysis of Concrete Gravity Dams Using Euler and Lagrange Approaches", PhD. Thesis, Karadeniz Technical University, Trabzon, Turkey.

Calayır, Y., Dumanoğlu, A.A. and Bayraktar, A. (1996), "Earthquake analysis of gravity dam–reservoir systems using the Eulerian and Lagrangian approaches", *Comput. Struct.*, **59**(5), 877-890.

Chen, B. and Yuan, Y. (2011), "Hydrodynamic pressures on arch dam during earthquakes", *J. Hydraul. Eng.*

- *ASCE*, **137**(1), 34-44.
Chopra, A.K. (1967), "Hydrodynamic pressures on dams during earthquake", *J. Eng. Mech. - ASCE*, **93**(6), 205-223.
Clough, R.W. and Penzien, J. (1975), " Dynamics of Structures", McGraw-Hill, New York, USA.
Cook, R.D., Malkus, D.S. and Plesha, M.E. (1989), "Concept and Applications of Finite Element Analysis", John Wiley and Sons., Singapore.
Degroote, J., Annerel, S. and Vierendeels, J. (2010), "Stability analysis of Gauss-Seidel iterations in a partitioned Simulation of fluid–structure interaction", *Comput. Struct.*, **88**(5-6), 263-271.
Fathi, A. and Lotfi, V. (2008), "Effects of reservoir length on dynamic analysis of concrete gravity dams", *Proceedings of the 14th World Conference on Earthquake Engineering*, Beijing, China.
Gogoi, I. and Maity, D. (2010), "A novel procedure for determination of hydrodynamic pressure along upstream face of dams due to earthquakes", *Comput. Struct.*, **88**(5-6), 539-548.
Heydari, M.M. and Mansoori, A. (2011), "Dynamic analysis of dam-reservoir interaction in time domain." *World. Appl. Sci. J.*, **15**(10), 1403-1408.
Lin, G., Wang, Y. and Hu, Z. (2012), "An efficient approach for frequency-domain and time-domain hydrodynamic analysis of dam–reservoir systems", *Earthq. Eng. Struct. Dyn.*, **41**(13), 1725-1749.
Miquel, B and Bouaanani, N. (2013), "Accounting for earthquake-induced dam-reservoir interaction using modified accelerograms", *J. Hydraul. Eng. - ASCE*, **139**(9), 1608-1617.
Samii, A. and Lotfi, V. (2007), "Comparison of coupled and decoupled modal approaches in seismic analysis of concrete gravity dams in time domain", *Finite. Elem. Anal. Des.*, **43**(13), 1003-1012.
Samii, A. and Lotfi, V. (2013), "A high-order based boundary condition for dynamic analysis of infinite reservoirs", *Comput. Struct.*, **120**, 65-76.
Sevim, B., Altunişik, A.C., Bayraktar, A., Akköse, M. and Calayir, Y. (2011a), "Water length and height effects on the earthquake behavior of arch dam-reservoir-foundation systems", *KSCE. J. Civil. Eng.*, **15**(2), 295-303.
Sevim, B., Bayraktar, A., Altunışık, A.C. (2011b), "Finite element model calibration of Berke arch dam using operational modal testing", *J. Vib. Control.*, **17**(7), 1065-1079.
Shariatmadar, H. and Mirhaj, A. (2011). "Dam-reservoir-foundation interaction effects on the modal characteristic of concrete gravity dams", *Struct. Eng. Mech.*, **38**(1), 65-79.
Wang, H., Feng, M. and Yang, H. (2012). " Seismic nonlinear analyses of a concrete gravity dam with 3D full dam model", *Bull. Earthq. Eng.*, **10**(6), 1959-1977.
Westergaard, H.M. (1933), "Water Pressures on Dams during Earthquakes", *Trans. Am. Soc. Civil. Eng.*, **98**(2), 418-433.
Wick, T. (2013), "Coupling of fully Eulerian and arbitrary Lagrangian-Eulerian methods for fluid-structure interaction computations", *Comput. Mech.*, **52**(5), 1113-1124.
Wilson, E.L. and Khalvati, M. (1983), "Finite elements for the dynamic analysis of fluid-solid systems", *Int. J. Numer. Method. Eng.*, **19**(11), 1657-1668.
Wood, C., Gil, A.J., Hassan, O. and Bonet, J. (2010). "Partitioned block-Gauss–Seidel coupling for dynamic fluid–structure interaction", *Comput. Struct.*, **88**(23-24), 1367-1382.
Zeinkiewicz, O.C. and Taylor, R.L. (1991), *Finite Element Method*, McGraw-Hill, London.

CC